Differentially expressed genes in ethanol extract of vanilla planifolia stem-induced cell death in glioblastoma cells

Hui Hua Chang
National Cheng Kung University
Yu-Ju Chen
Chang Jung Christian University
Sung-Ghun Wu
Chang Jung Christian University
Li-Jyun Chen
Kaohsiung Medical University
Bing-Chen Tsai
National Cheng Kung University
Yuan-Shuo Hsueh (yshsueh@kmu.edu.tw)
Kaohsiung Medical University

Research Article

Keywords: Glioblastoma multiforme, vanilla planifolia, RNA-seq, differentially expressed genes, therapeutic targets

Posted Date: November 14th, 2023

DOI: https://doi.org/10.21203/rs.3.rs-3531938/v1

Additional Declarations: No competing interests reported.

Abstract

Purpose

Glioblastoma multiforme (GBM) is a highly malignant brain tumor with poor prognosis after conventional treatment. Therefore, novel therapeutic targets and potential treatment strategies have gained increased attention. Vanilla planifolia is an original source for vanilla flavoring due to its high vanillin content. Several studies have proven the antitumor activity of vanillin in colon cancer.

Methods

In this study, three GBM cell lines, patient-derived temozolomide (TMZ)-resistant GBM P#5 TMZ-R cells, T98G cells, and U-87 MG cells, were used to evaluate the antitumor activity of extracts from vanilla planifolia.

Results

Our data showed that ethanol extract of vanilla planifolia stem (VAS) at 200 ng/μl significantly reduced cell viability and colony formation of GBM cells. Moreover, VAS induced MAP1LC3 cleavage, a marker of autophagy. Further RNA-seq analysis and MA plot showed 1972 upregulated differentially expressed genes (DEGs) and 2276 downregulated DEGs in 200 ng/μl VAS-treated P#5 TMZ-R cells compared to the control. Protein-protein interaction between fold change of DEGs less than − 3 and over 5 were further analyzed, and we found that 16 and 9 hub DEGs, respectively, were correlated with other DEGs. Further qPCR experiments showed that the mRNA expression of *DHRS9, HOPX, AQP5, PCP4, RGS8, GNAT2, RLBP1, FA2H, TNMD, SKAP1, MATN1, IGFBP1, ELFN2, and C2CD4C* was significantly downregulated. Moreover, the expression of *IL36RN, CCL20, CCL5, CXCL10, HMOX1, MX2, RSAD2, IFI44L*, and *EGR1* was significantly upregulated.

Conclusion

These findings demonstrated that VAS reduced cell viability and colony formation, induced autophagy, and pinpointed some hub DEGs as potential therapeutic targets for GBM treatment.

Introduction

Glioblastoma multiforme (GBM) is the most common and malignant brain tumor in adults [1, 2]. According to the classification of the World Health Organization (WHO), GBM is defined as grade IV astrocytoma, which has the highest malignancy and aggressiveness [3]. Although the incidence rate of GBM is relatively low, the poor overall survival and high mortality after conventional surgery, chemotherapy, and radiotherapy have attracted researchers' attention [4, 5]. According to The Cancer

Genome Atlas (TCGA) database, GBM is characterized by aberrant amplification or mutation of EGFR, PDGFRA, CDK4, NF1, HER2, TP53, PIK3R1, and TERT [6, 7]. These findings attracted scientists' attention to evaluate several inhibitors against EGFR or PDGFRA in vitro and in vivo for GBM treatment. Unfortunately, these clinical trials of EGFR inhibitors or PDGFRA inhibitors in GBM patients failed [8–12]. Several potential targets, such as HSP90 and HDAC, and their specific inhibitors have been proven to have antitumor activities in GBM cells [13, 14]. It is still urgent to explore a potential treatment for GBM.

Vanilla planifolia, a type of vanilla orchid, is a major source of vanilla flavoring due to its high vanillin content [15]. Vanillin is widely used as a crucial flavor and aromatic component in global cuisine. Numerous studies have explored its various functions, including its potential as an antitumor agent. Ho et al. and Ramadoss et al. have shown that vanillin can induce apoptosis and halt the cell cycle in colon cancer [16, 17]. Other studies revealed that vanillin interacts with calcium/calmodulin-dependent protein kinase IV and microtubule affinity-regulated kinase 4, leading to mitochondrial damage, reactive oxygen species production, and apoptosis [18, 19]. Vanillin could modulate signaling pathways of PI3K, NFKB, and STAT3/HIF1A, and inhibits cell invasion and metastasis [20–23]. Furthermore, vanillin has been found to synergistically enhance the anticancer effects of cisplatin and doxorubicin [24, 25]. Despite recognizing the anticancer potential of vanillin, the detailed molecular mechanism underlying its tumor-suppressive effects remains to be fully elucidated.

In this study, we aimed to evaluate the antitumor activity of vanilla planifolia on GBM cells. The leaves, stems, and pods of vanilla planifolia were extracted by ethanol or water. Three GBM cell lines, patient-derived temozolomide (TMZ)-resistant GBM P#5 TMZ-R cells, T98G cells, and U-87 MG cells, were used to evaluate the antitumor activity of the ethanol extract of vanilla planifolia stem (VAS). Then, RNA-seq was performed to explore the differentially expressed genes (DEGs) between control and VAS-treated cells. Further qPCR was used to validate the findings of RNA-seq. Our data showed that VAS reduced cell viability and colony formation in GBM cells. Moreover, VAS induced MAP1LC3 cleavage and altered the expression of genes involved in the cell cycle, apoptosis, and autophagy. Further RNA-seq experiments pinpoint that these DEGs may play important roles in VAS-induced cell death and are potential therapeutic targets for GBM treatment.

Materials and Methods

Extraction of Vanilla planifolia

Vanilla planifolia was planted and provided by Shing-Kuan Wu (Chang Jung Christian University). The leaves, stems, and pods of vanilla planifolia were harvested and extracted by ethanol or water. The extracts were filtrated and evaporated using a rotary evaporator. The crude extracts underwent a freeze-drying process to ensure that the sample was free of water. The crude extracts of ethanol and water were resolved in DMSO and ddH_2O, respectively.

Cell Culture, chemicals, and antibodies

The U-87 MG and T98G GBM cell lines were purchased from BCRC (#60360, Taiwan) and JCRB (JCRB9041, Japan), respectively. P#5 TMZ-R, a patient-derived GBM cell line with temozolomide resistance, were kindly provided by Dr. Jian Ying Chuang (Taipei Medical University, Taiwan). In accordance with a previous study, cells were cultured in Dulbecco's modified Eagle's medium (DMEM) supplemented with 10% fetal bovine serum (FBS, HyClone, USA), 100 U/ml penicillin, and 0.1 mg/ml streptomycin (GeneDirex, Taiwan), and maintained in a humidified incubator at 37°C with 5% CO_2 [13]. Specific antibodies against MAP1LC3 (Cell Signaling Technology, Danvers, MA) and GAPDH (Santa Cruz Biotechnology, Dallas, TX) were used.

Cell viability assay

This assay was performed following previous study [26]. Cells in a 24-well plates were exposed to ethanol or water extracts of vanilla planifolia at the specified doses. After five days, cells were stained with methylene blue dye. The dye was dissolved and measured at a wavelength of 595 nm by a SpectraMax iD3 Microplate Reader (Molecular Devices). Cell viability was assessed by measuring the absorbance and normalizing it to the DMSO-only control group. Each experimental data point was obtained from triplicate wells within each plate and replicated in a minimum of three plates. The data are presented as the mean ± standard error of the mean (SEM).

Colony formation assay

This assay was performed following previous study [26]. After seeding cells in 6-well plates, they were treated with extracts for 24 hours. The medium was refreshed with growth medium without extracts, and the cells were incubated for two weeks. Colonies were visualized by staining with 0.5% methylene blue, and the number of colonies was determined and normalized to the control group.

Immunoblotting

This assay was performed following previous study [26]. Cells were lysed with CelLyticTM M cell lysis buffer, which contained protease inhibitors and phosphatase inhibitors. The protein concentration was determined using the Bio-Rad® protein assay dye reagent concentrate (Cat. #500-0006). Equal amounts of total protein were denatured, separated by sodium dodecyl sulfate-polyacrylamide gel electrophoresis (SDS-PAGE), and transferred to PVDF membranes. The specific proteins on the PVDF membrane were identified by primary antibodies and HRP-conjugated secondary antibodies, and were visualized using enhanced chemiluminescence (ECL) reagents (PerkinElmer) and captured using an iBright imaging system (Thermo Fisher Scientific®). The band density was analyzed using ImageJ software.

RNA extraction

The procedure followed the standard protocol of the Quick-RNA™ Miniprep Kit (ZYMO RESEARCH®). Briefly, TRIzol Reagent was used to lyse VAS-treated cells. Total RNA was then purified using Zymo-Spin™ columns and quantified using NanoDrop™ spectrophotometers (Thermo Fisher Scientific®).

RNA sequencing and bioinformatic analysis

RNA sequencing was performed by Genomics Inc. (Taiwan) using Illumina NovaSeq platforms following previous study [14]. The quality of the RNA was assessed by calculating RNA integrity number (RIN) scores using an Agilent 2100 Bioanalyzer. The sequenced RNA was aligned to the human genome (hg19). Gene expression levels were quantified using RSEM software. Differentially expressed genes (DEGs) were identified using EBSeq at a target false discovery rate (FDR) of 0.05. Gene Ontology (GO) enrichment analysis and Kyoto Encyclopedia of Genes and Genomes (KEGG) pathway analysis were conducted. Additionally, the protein-protein interaction (PPI) network of DEGs was visualized using the STRING website (https://string-db.org/cgi/input?sessionId=bBRBaHkRJB8j&input_page_show_search=on) to gain insights into the involvement of these genes.

Quantitative analysis of mRNA

One μg of total RNA and the ReverTra Ace Set (PURIGO, Taiwan) were used to synthesis cDNA. For mRNA expression quantification, real-time PCR (qPCR) was performed using THUNDERBIRD® SYBR® qPCR Mix (TOYOBO, Japan) and analyzed by StepOnePlus™ Real-Time PCR System (Thermo Fisher Scientific®). The primers used for qPCR can be found in Table S1. Each experiment was conducted in triplicate, and the data are presented as the mean ± standard error of the mean (SEM).

Statistical analyses

The data were analyzed using the Statistical Package for the Social Sciences (SPSS, Inc.), version 16 for Windows. All data are presented as the mean ± standard error of the mean (SEM). A one-way analysis of variance (ANOVA) was conducted to compare the means among different groups, followed by a Bonferroni post hoc test. Statistical significance was determined at the $*p < 0.05$ level.

Results

Vanilla planifolia stems extracted by ethanol reduces viability and colony formation and induces autophagy in GBM cells.

In this study, three GBM cell lines were used to evaluate the antitumor activities of ethanol extract and water extract from vanilla planifolia, including patient-derived temozolomide (TMZ)-resistant GBM P#5 TMZ-R cells, T98G cells, and U-87 MG cells. First, P#5 TMZ-R cells were treated with the pods, leaves, and stems of vanilla planifolia crude extracts of ethanol and water at 50 and 100 ng/μl. Figure 1A shows that the ethanol extract and water extract of vanilla planifolia pods and leaves only had slightly inhibitory effects. Interestingly, ethanol extract of vanilla planifolia stem (VAS) significantly reduced the cell viability of P#5 TMZ-R at 50 and 100 ng/μl, but the water extract of vanilla planifolia stems did not inhibit the cell viability. Then, to explore the IC_{50}, the cells were further treated with VAS at 50, 100, 150, and 200 ng/μl. Figure 1B shows that VAS effectively inhibited the viability of P#5 TMZ-R cells (IC_{50}: 137 ng/μl), T98G

cells (IC_{50}: 150 ng/μl), and U-87 MG cells (IC_{50}: 168 ng/μl). Furthermore, 200 ng/μl VAS significantly inhibited colony formation in P#5 TMZ-R, T98G, and U-87 MG cells (Fig. 1C and **D**). To further examine the cell death pathway after 200 ng/μl VAS treatment for 72 h, our data showed that MAP1LC3-II conversion was a more robust readout than the control in P#5 TMZ-R, T98G, and U-87 MG cells (Fig. 2A and **B**). Taken together, these data indicate that VAS treatment induced autophagy and reduced the viability and colony formation of GBM cells.

VAS led to 4248 differentially expressed genes in GBM cells.

Next, to verify which VAS-mediated genes led to cell death, RNA-seq was used to measure mRNA expression after VAS treatment. Based on our findings, the cells were treated with 200 ng/μl VAS and analyzed by RNA-seq. The transcripts were compared between 200 ng/μl VAS and the vehicle control. The volcano plot and MA plot of DEGs between the two groups are shown in Fig. 3A and **B**. Compared with the vehicle control, 1972 DEGs were upregulated ($p < 0.05$, log2-fold change > 1), and 2276 DEGs were downregulated ($p < 0.05$, log2-fold change < -1). Then, we used KEGG enrichment and GO to determine the functional annotation of these genes to investigate the involvement of expressed DEGs after VAS treatment in biological process (BP), molecular function (MF), and cellular component (CC). KEGG analysis showed that the cell cycle, apoptosis, cellular senescence, autophagy, and lysosome were the top five enriched terms (Fig. 3C). GO analysis showed that in BP enrichment analysis, spindle organization, DNA replication, and macroautophagy were the top three enriched terms (Fig. 3D). In the MF category of GO analysis, small GTPase binding, GTPase binding, ubiquitin-like or ubiquitin protein ligase binding, and cadherin were the top enriched terms (Fig. 3E). The terms associated with CC may be linked with chromosomal region, nuclear envelope, and spindle (Fig. 3F). Taken together, these enrichment analysis results implied that VAS affected critical functions and pathways for survival and proliferation in GBM cells.

To further explore the most important DEG clustering of GBM survival after VAS treatment, we constructed a protein–protein interaction (PPI) network. Eight-nine downregulated DEGs with log2-fold change < -3 were analyzed by the STRING database, and 16 hub DEGs were correlated, including *TNMD, MATN1, RLBP1, IGFBP1, PCP4, DHRS9, GNAT2, C2CD4C, ELFN2, GDA, AQP5, SKAP1, HOPX, PLCB2, FA2H*, and *RGS8* (Fig. 4A). The fold changes in these hub DEGs determined by RNA-seq are shown in Fig. 4B. Similarly, nine upregulated DEGs in twenty-three DEGs with log2-fold change > 5 showed correlation using STRING analysis, including *CXCL10, IL36RN, MX2, EGR1, RSAD2, CCL5, IFI44L, CCL20*, and *HMOX1* (Fig. 4C). The fold changes in these upregulated DEGs determined by RNA-seq are shown in Fig. 4D.

VAS significantly downregulated 14 DEGs and upregulated 9 DEGs by qPCR in GBM cells.

To further validate the expression of these hub DEGs, a qPCR experiment was performed in P#5 TMZ-R cells and U-87 MG cells. Figure 5A shows that the mRNA expression levels of *TNMD, MATN1, RLBP1, IGFBP1, PCP4, DHRS9, GNAT2, C2CD4C, ELFN2, AQP5, SKAP1, HOPX, FA2H*, and *RGS8* were significantly reduced after VAS treatment in both P#5 TMZ-R cells and U-87 MG cells. Moreover, VAS also significantly

induced the mRNA expression of *CXCL10, IL36RN, MX2, EGR1, RSAD2, CCL5, IFI44L, CCL20*, and *HMOX1* in both P#5 TMZ-R cells and U-87 MG cells. (Fig. 5B). Taken together, these findings implied that VAS could influence the expression of numerous genes and mediate cell death in GBM cells.

Discussion

In the present study, we found that ethanol extract and water extract of vanilla planifolia pods and leaves did not show obvious inhibitory effects. The water extract of the vanilla planifolia stems had little inhibitory effect on cell viability. Interestingly, VAS significantly reduced the viability and colony formation of GBM cells. VAS also induced MAP1LC3B cleavage, suggesting that VAS-induced cell death might occur via autophagy activation. Further RNA-seq analysis after VAS treatment showed that the levels of 1972 DEGs were upregulated and those of 2276 DEGs were downregulated. KEGG and GO analyses pinpointed that these DEGs were involved in the cell cycle, apoptosis, autophagy, spindle organization, and DNA replication. Further analysis of protein–protein interactions with fold changes of DEGs less than − 3 and over 5 showed 16 and 9 hub DEGs, respectively. Further qPCR experiments showed that 14 hub DEGs were significantly downregulated and 9 hub DEGs were significantly upregulated.

These 14 downregulated hub DEGs after VAS treatment included *TNMD, MATN1, RLBP1, IGFBP1, PCP4, DHRS9, GNAT2, C2CD4C, ELFN2, AQP5, SKAP1, HOPX, FA2H*, and *RGS8*. Some literature has shown the correlation of these hub genes with cancers. Rakha et al. showed that the expression level of retinaldehyde binding protein 1 (RLBP1) was associated with tumor grade in invasive breast cancer [27]. High insulin-like growth factor binding protein 1 (IGFBP1) expression was significantly associated with poorer survival and relapse-free survival in patients with gastric cancer [28]. Purkinje cell protein 4 (PCP4), also called PEP19, has been demonstrated to promote migration, invasion and adhesion in human breast cancer MCF-7 and T47D cells [29]. Dehydrogenase/reductase 9 (DHRS9) overexpression was correlated with poor response to concurrent chemoradiotherapy and poor prognosis in rectal cancer patients [30]. Extracellular leucine rich repeat and fibronectin type III domain containing 2 (ELFN2) was highly expressed in astrocytoma patients and significantly correlated with their overall survival [31]. The expression level of aquaporin 5 (AQP5) in breast cancer was associated with lymph node metastasis and poor prognosis [32]. In a transcriptome-wide association study, low src kinase-associated phosphoprotein 1 (SKAP1) expression in blood increased endometrial cancer risk [33]. Homeodomain-only protein homeobox (HOPX) downregulation by epigenetic regulation leads to cancer aggressiveness in breast cancer [34]. Dai et al. found that fatty acid 2-hydroxylase (FA2H) was underexpressed in triple-negative breast cancers both in vitro and in the clinic [35]. They also further demonstrated that FA2H suppressed cancer stemness in breast cancers by inhibiting the STAT3/IL6 axis and NFkB signaling. The mRNA and protein expression levels of regulator of G protein signaling 8 (RGS8) in normal tissues were higher than those in thyroid carcinoma tissues [36]. Bai et al. also showed that higher expression of RGS8 in patients with thyroid carcinoma was associated with better survival outcomes.

In addition to downregulated hub DEGs, VAS also induced 9 hub DEGs, including *CXCL10, IL36RN, MX2, EGR1, RSAD2, CCL5, IFI44L, CCL20*, and *HMOX1*. The CXCL9, -10, -11/CXCR3 axis has been demonstrated

to regulate immune cell migration, differentiation, and activation, leading to tumor suppression [37]. Interleukin 36 receptor antagonist (IL36RN) can inhibit the activity of interleukin-36 by binding to its receptor IL1RL2 and mediating inflammation. The expression of IL-36 family member mRNA and protein is significantly increased in colorectal cancer tissue compared to adjacent nontumor tissues [38]. MX2 was obviously downregulated in both GBM patients and GBM cell lines [39]. Moreover, MX2 overexpression markedly reduced the proliferation, migration, and invasion of glioma cells. Early growth response-1 (EGR1) downregulation in prostate cancer cells reduced both the number and size of metastases but did not affect tumor growth, implying that EGR1 regulates angiogenic factors and promotes metastasis [40]. TCGA gene expression profile and Kaplan–Meier analysis showed that high expression of radical s-adenosyl methionine domain containing 2 (RSAD2) in patients with oral cancer was associated with a better prognosis [41]. Melese et al. found that targeting CCL5 or CCL5 receptors on immunosuppressive cells to alter the immune microenvironment promoted lung cancer progression and immunotherapy insensitivity [42]. In the clinic, the expression level of interferon-induced protein 44-like (IFI44L) is significantly reduced in HCC tumor tissues [43]. Low expression of IFI44L levels also correlated with larger tumor size, disease relapse, advanced stages, and poor clinical survival in HCC patients. The CCL20-CCR6 axis promotes cancer progression directly by enhancing the migration and proliferation of cancer cells and indirectly by remodeling the tumor microenvironment through immune cell control [44]. HMOX1 is highly expressed in a variety of cancers, including lung, breast, colorectal, and glioblastoma [45, 46]. Taken together, these hub DEGs deserve further exploration of their roles as biomarkers or therapeutic targets in GBM cells.

Conclusion

In conclusion, we found that the ethanol extract of vanilla planifolia stems significantly reduced the viability and colony formation of P#5 TMZ-R, T98G, and U-87 MG cells. The increase in MAP1LC3 cleavage indicates that VAS treatment induces autophagy in all three GBM cell lines. According to the RNA-seq data and bioinformatics analysis, such as KEGG and GO, we found that VAS affected critical functions and pathways for survival and proliferation in GBM cells. Protein–protein interaction analysis highlighted 16 downregulated hub DEGs and 9 upregulated hub DEGs. Further validation of these hub DEGs by qPCR showed that *DHRS9, HOPX, AQP5, PCP4, RGS8, GNAT2, RLBP1, FA2H, TNMD, SKAP1, MATN1, IGFBP1, ELFN2*, and *C2CD4C* were significantly downregulated. Furthermore, the mRNA expression of *IL36RN, CCL20, CCL5, CXCL10, HMOX1, MX2, RSAD2, IFI44L*, and *EGR1* was significantly upregulated. Taken together, VAS shows antitumor activity in GBM cells. Moreover, these VAS-mediated hub DEGs may be potential therapeutic targets for GBM treatment.

Abbreviations

GBM: Glioblastoma multiforme; TMZ: Temozolomide; VAS: Ethanol extract of vanilla planifolia stem; DEGs: Differentially expressed genes; GO: Gene ontology; KEGG: Kyoto Encyclopedia of Genes and

Genomes; PPI: Protein–protein interaction; BP: Biological process; MF: Molecular function; CC: Cellular component.

Declarations

Acknowledgments

We would like to thank Chih-Ying Lin (Institute of Clinical Pharmacy and Pharmaceutical Sciences, College of Medicine, National Cheng Kung University National Cheng Kung University) for administrative support.

Author contributions

YSH developed the study concept. The data curation and formal analysis were performed by YJC, SGW, LJC, and BCT. HHC and YSH provided the funding acquisition and supervised the study, and wrote the manuscript. All authors read and approved the final manuscript.

Funding

This work was supported by Chang Jung Christian University, the Ministry of Science and Technology (MOST 110-2314-B-309-001, MOST 109-2314-B-309-002), and National Science and Technology Council (NSTC 111-2314-B-309-001, NSTC 111-2628-B-006-010-MY3) in Executive Yuan, Taiwan.

Availability of data and materials

The original contributions presented in the study are included in the article. Additional files, further inquiries can be directed to the corresponding author.

Ethics approval and consent to participate

Not applicable.

Consent for publication

Not applicable.

Competing interests

All authors declare no potential conflicts of interest.

References

1. Davis FG, McCarthy BJ. Current epidemiological trends and surveillance issues in brain tumors. Expert Rev Anticancer Ther. 2001;1:395–401. 10.1586/14737140.1.3.395.

2. Jansen M, Yip S, Louis DN. Molecular pathology in adult gliomas: diagnostic, prognostic, and predictive markers. Lancet Neurol. 2010;9:717–26. 10.1016/S1474-4422(10)70105-8.
3. Louis DN, Perry A, Reifenberger G, von Deimling A, Figarella-Branger D, Cavenee WK, Ohgaki H, Wiestler OD, Kleihues P, Ellison DW. The 2016 World Health Organization Classification of Tumors of the Central Nervous System: a summary. Acta Neuropathol. 2016;131:803–20. 10.1007/s00401-016-1545-1.
4. Soderberg-Naucler C, Rahbar A, Stragliotto G. Survival in patients with glioblastoma receiving valganciclovir. N Engl J Med. 2013;369:985–6. 10.1056/NEJMc1302145.
5. Wen PY, Kesari S. Malignant gliomas in adults. N Engl J Med. 2008;359:492–507. 10.1056/NEJMra0708126.
6. Szerlip NJ, Pedraza A, Chakravarty D, Azim M, McGuire J, Fang Y, Ozawa T, Holland EC, Huse JT, Jhanwar S, Leversha MA, Mikkelsen T, Brennan CW. Intratumoral heterogeneity of receptor tyrosine kinases EGFR and PDGFRA amplification in glioblastoma defines subpopulations with distinct growth factor response. Proc Natl Acad Sci U S A. 2012;109:3041–6. 10.1073/pnas.1114033109.
7. Brennan CW, Verhaak RG, McKenna A, Campos B, Noushmehr H, Salama SR, Zheng S, Chakravarty D, Sanborn JZ, Berman SH, Beroukhim R, Bernard B, Wu CJ, Genovese G, Shmulevich I, Barnholtz-Sloan J, Zou L, Vegesna R, Shukla SA, Ciriello G, Yung WK, Zhang W, Sougnez C, Mikkelsen T, Aldape K, Bigner DD, Van Meir EG, Prados M, Sloan A, Black KL, Eschbacher J, Finocchiaro G, Friedman W, Andrews DW, Guha A, Iacocca M, O'Neill BP, Foltz G, Myers J, Weisenberger DJ, Penny R, Kucherlapati R, Perou CM, Hayes DN, Gibbs R, Marra M, Mills GB, Lander E, Spellman P, Wilson R, Sander C, Weinstein J, Meyerson M, Gabriel S, Laird PW, Haussler D, Getz G, Chin L, Network TR. The somatic genomic landscape of glioblastoma. Cell. 2013;155:462–77. 10.1016/j.cell.2013.09.034.
8. Kwatra MM. A Rational Approach to Target the Epidermal Growth Factor Receptor in Glioblastoma. Curr Cancer Drug Targets. 2017;17:290–6. 10.2174/1568009616666161227091522.
9. Karpel-Massler G, Schmidt U, Unterberg A, Halatsch ME. Therapeutic inhibition of the epidermal growth factor receptor in high-grade gliomas: where do we stand? Mol Cancer Res. 2009;7:1000–12. 10.1158/1541-7786.MCR-08-0479.
10. Brandes AA, Franceschi E, Tosoni A, Hegi ME, Stupp R. Epidermal growth factor receptor inhibitors in neuro-oncology: hopes and disappointments. Clin Cancer Res. 2008;14:957–60. 10.1158/1078-0432.CCR-07-1810.
11. Pastorino S, Langley EJ, Chao Y, Jiang P, Mukthavaram R, Pingle SC, Kim PS, Singh S, Kesari S. Mechanisms of resistance to PDGFR inhibition in glioblastoma. J Clin Oncol. 2014;32:e13030–0. 10.1200/jco.2014.32.15_suppl.e13030.
12. Padfield E, Ellis HP, Kurian KM. Current Therapeutic Advances Targeting EGFR and EGFRvIII in Glioblastoma. Front Oncol. 2015;5:5. 10.3389/fonc.2015.00005.
13. Ho KT, Chen PF, Chuang JY, Gean PW, Hsueh YS. A heat shock protein 90 inhibitor reduces oncoprotein expression and induces cell death in heterogeneous glioblastoma cells with EGFR, PDGFRA, CDK4, and NF1 aberrations. Life Sci. 2021;288:120176. 10.1016/j.lfs.2021.120176.

14. Chang HH, Chang YY, Tsai BC, Chen LJ, Chang AC, Chuang JY, Gean PW, Hsueh YS. A Selective Histone Deacetylase Inhibitor Induces Autophagy and Cell Death via SCNN1A Downregulation in Glioblastoma Cells. Cancers (Basel). 2022;14:4537. 10.3390/cancers14184537.
15. Priefert H, Rabenhorst J, Steinbuchel A. Biotechnological production of vanillin. Appl Microbiol Biotechnol. 2001;56:296–314. 10.1007/s002530100687.
16. Ho K, Yazan LS, Ismail N, Ismail M. Apoptosis and cell cycle arrest of human colorectal cancer cell line HT-29 induced by vanillin. Cancer Epidemiol. 2009;33:155–60. 10.1016/j.canep.2009.06.003.
17. Ramadoss DP, Sivalingam N. Vanillin extracted from Proso and Barnyard millets induce apoptotic cell death in HT-29 human colon cancer cell line. Nutr Cancer. 2020;72:1422–37. 10.1080/01635581.2019.1672763.
18. Naz H, Tarique M, Khan P, Luqman S, Ahamad S, Islam A, Ahmad F, Hassan MI. Evidence of vanillin binding to CAMKIV explains the anti-cancer mechanism in human hepatic carcinoma and neuroblastoma cells. Mol Cell Biochem. 2018;438:35–45. 10.1007/s11010-017-3111-0.
19. Khan P, Rahman S, Queen A, Manzoor S, Naz F, Hasan GM, Luqman S, Kim J, Islam A, Ahmad F, Hassan MI. Elucidation of Dietary Polyphenolics as Potential Inhibitor of Microtubule Affinity Regulating Kinase 4: In silico and In vitro Studies. Sci Rep. 2017;7:9470. 10.1038/s41598-017-09941-4.
20. Liang JA, Wu SL, Lo HY, Hsiang CY, Ho TY. Vanillin inhibits matrix metalloproteinase-9 expression through down-regulation of nuclear factor-kappaB signaling pathway in human hepatocellular carcinoma cells. Mol Pharmacol. 2009;75:151–7. 10.1124/mol.108.049502.
21. Lirdprapamongkol K, Kramb JP, Suthiphongchai T, Surarit R, Srisomsap C, Dannhardt G, Svasti J. Vanillin suppresses metastatic potential of human cancer cells through PI3K inhibition and decreases angiogenesis in vivo. J Agric Food Chem. 2009;57:3055–63. 10.1021/jf803366f.
22. Lirdprapamongkol K, Sakurai H, Kawasaki N, Choo MK, Saitoh Y, Aozuka Y, Singhirunnusorn P, Ruchirawat S, Svasti J, Saiki I. Vanillin suppresses in vitro invasion and in vivo metastasis of mouse breast cancer cells. Eur J Pharm Sci. 2005;25:57–65. 10.1016/j.ejps.2005.01.015.
23. Park EJ, Lee YM, Oh TI, Kim BM, Lim BO, Lim JH. Vanillin Suppresses Cell Motility by Inhibiting STAT3-Mediated HIF-1alpha mRNA Expression in Malignant Melanoma Cells. Int J Mol Sci. 2017;18:532. 10.3390/ijms18030532.
24. Durant S, Karran P. Vanillins–a novel family of DNA-PK inhibitors. Nucleic Acids Res. 2003;31:5501–12. 10.1093/nar/gkg753.
25. Elsherbiny NM, Younis NN, Shaheen MA, Elseweidy MM. The synergistic effect between vanillin and doxorubicin in ehrlich ascites carcinoma solid tumor and MCF-7 human breast cancer cell line. Pathol Res Pract. 2016;212:767–77. 10.1016/j.prp.2016.06.004.
26. Hsueh YS, Chang HH, Shan YS, Sun HS, Fletcher JA, Li CF, Chen LT. Nuclear KIT induces a NFKBIB-RELA-KIT autoregulatory loop in imatinib-resistant gastrointestinal stromal tumors. Oncogene. 2019;38:6550–65. 10.1038/s41388-019-0900-9.

27. Schackert G, Simmons RD, Buzbee TM, Hume DA, Fidler IJ. Macrophage infiltration into experimental brain metastases: occurrence through an intact blood-brain barrier. J Natl Cancer Inst. 1988;80:1027–34. 10.1093/jnci/80.13.1027.
28. Sato Y, Inokuchi M, Takagi Y, Kojima K. IGFBP1 Is a Predictive Factor for Haematogenous Metastasis in Patients With Gastric Cancer. Anticancer Res. 2019;39:2829–37. 10.21873/anticanres.13411.
29. Yoshimura T, Hamada T, Hijioka H, Souda M, Hatanaka K, Yoshioka T, Yamada S, Tsutsui M, Umekita Y, Nakamura N, Tanimoto A. PCP4/PEP19 promotes migration, invasion and adhesion in human breast cancer MCF-7 and T47D cells. Oncotarget. 2016;7:49065–74. 10.18632/oncotarget.7529.
30. Chen TJ, Hsu BH, Lee SW, Yang CC, Tian YF, Kuo YH, Li WS, Tsai HH, Wu LC, Yeh CF, Chou CL, Lai HY. Overexpression of Dehydrogenase/Reductase 9 Predicts Poor Response to Concurrent Chemoradiotherapy and Poor Prognosis in Rectal Cancer Patients. Pathol Oncol Res. 2022;28:1610537. 10.3389/pore.2022.1610537.
31. Liu C, Fu H, Liu X, Lei Q, Zhang Y, She X, Liu Q, Liu Q, Sun Y, Li G, Wu M. LINC00470 Coordinates the Epigenetic Regulation of ELFN2 to Distract GBM Cell Autophagy. Mol Ther. 2018;26:2267–81. 10.1016/j.ymthe.2018.06.019.
32. Bystrup M, Login FH, Edamana S, Borgquist S, Tramm T, Kwon TH, Nejsum LN. Aquaporin-5 in breast cancer. APMIS. 2022;130:253–60. 10.1111/apm.13212.
33. Canson DM, O'Mara TA, Spurdle AB, Glubb DM. Splicing annotation of endometrial cancer GWAS risk loci reveals potentially causal variants and supports a role for NF1 and SKAP1 as susceptibility genes. HGG Adv. 2023;4:100185. 10.1016/j.xhgg.2023.100185.
34. Kikuchi M, Katoh H, Waraya M, Tanaka Y, Ishii S, Tanaka T, Nishizawa N, Yokoi K, Minatani N, Ema A, Kosaka Y, Tanino H, Yamashita K, Watanabe M. Epigenetic silencing of HOPX contributes to cancer aggressiveness in breast cancer. Cancer Lett. 2017;384:70–8. 10.1016/j.canlet.2016.10.017.
35. Dai X, Zhang S, Cheng H, Cai D, Chen X, Huang Z. FA2H Exhibits Tumor Suppressive Roles on Breast Cancers via Cancer Stemness Control. Front Oncol. 2019;9:1089. 10.3389/fonc.2019.01089.
36. Bai M, Ke S, Yu H, Xu Y, Yu Y, Lu S, Wang C, Huang J, Ma Y, Dai W, Wu Y. Key molecules associated with thyroid carcinoma prognosis: A study based on transcriptome sequencing and GEO datasets. Front Immunol. 2022;13:964891. 10.3389/fimmu.2022.964891.
37. Tokunaga R, Zhang W, Naseem M, Puccini A, Berger MD, Soni S, McSkane M, Baba H, Lenz HJ. CXCL9, CXCL10, CXCL11/CXCR3 axis for immune activation - A target for novel cancer therapy. Cancer Treat Rev. 2018;63:40–7. 10.1016/j.ctrv.2017.11.007.
38. Baker K, O'Donnell C, Bendix M, Keogh S, Byrne J, O'Riordain M, Neary P, Houston A, Brint E. IL-36 signalling enhances a pro-tumorigenic phenotype in colon cancer cells with cancer cell growth restricted by administration of the IL-36R antagonist. Oncogene. 2022;41:2672–84. 10.1038/s41388-022-02281-2.
39. Wang H, Guan Q, Nan Y, Ma Q, Zhong Y. Overexpression of human MX2 gene suppresses cell proliferation, migration, and invasion via ERK/P38/NF-kappaB pathway in glioblastoma cells. J Cell Biochem. 2019;120:18762–70. 10.1002/jcb.29189.

40. Li L, Ameri AH, Wang S, Jansson KH, Casey OM, Yang Q, Beshiri ML, Fang L, Lake RG, Agarwal S, Alilin AN, Xu W, Yin J, Kelly K. EGR1 regulates angiogenic and osteoclastogenic factors in prostate cancer and promotes metastasis. Oncogene. 2019;38:6241–55. 10.1038/s41388-019-0873-8.
41. Reyimu A, Chen Y, Song X, Zhou W, Dai J, Jiang F. Identification of latent biomarkers in connection with progression and prognosis in oral cancer by comprehensive bioinformatics analysis. World J Surg Oncol. 2021;19:240. 10.1186/s12957-021-02360-w.
42. Melese ES, Franks E, Cederberg RA, Harbourne BT, Shi R, Wadsworth BJ, Collier JL, Halvorsen EC, Johnson F, Luu J, Oh MH, Lam V, Krystal G, Hoover SB, Raffeld M, Simpson RM, Unni AM, Lam WL, Lam S, Abraham N, Bennewith KL, Lockwood WW. CCL5 production in lung cancer cells leads to an altered immune microenvironment and promotes tumor development. Oncoimmunology. 2022;11:2010905. 10.1080/2162402X.2021.2010905.
43. Huang WC, Tung SL, Chen YL, Chen PM, Chu PY. IFI44L is a novel tumor suppressor in human hepatocellular carcinoma affecting cancer stemness, metastasis, and drug resistance via regulating met/Src signaling pathway. BMC Cancer. 2018;18:609. 10.1186/s12885-018-4529-9.
44. Kadomoto S, Izumi K, Mizokami A. The CCL20-CCR6 Axis in Cancer Progression. Int J Mol Sci. 2020;21:5186. 10.3390/ijms21155186.
45. Cameron BF, Zucker R, Harkness DR. Oxygen binding to human erythrocyte cell populations. Ann N Y Acad Sci. 1975;244:60–71. 10.1111/j.1749-6632.1975.tb41522.x.
46. Luu Hoang KN, Anstee JE, Arnold JN. The Diverse Roles of Heme Oxygenase-1 in Tumor Progression. Front Immunol. 2021;12:658315. 10.3389/fimmu.2021.658315.

Figures

Figure 1

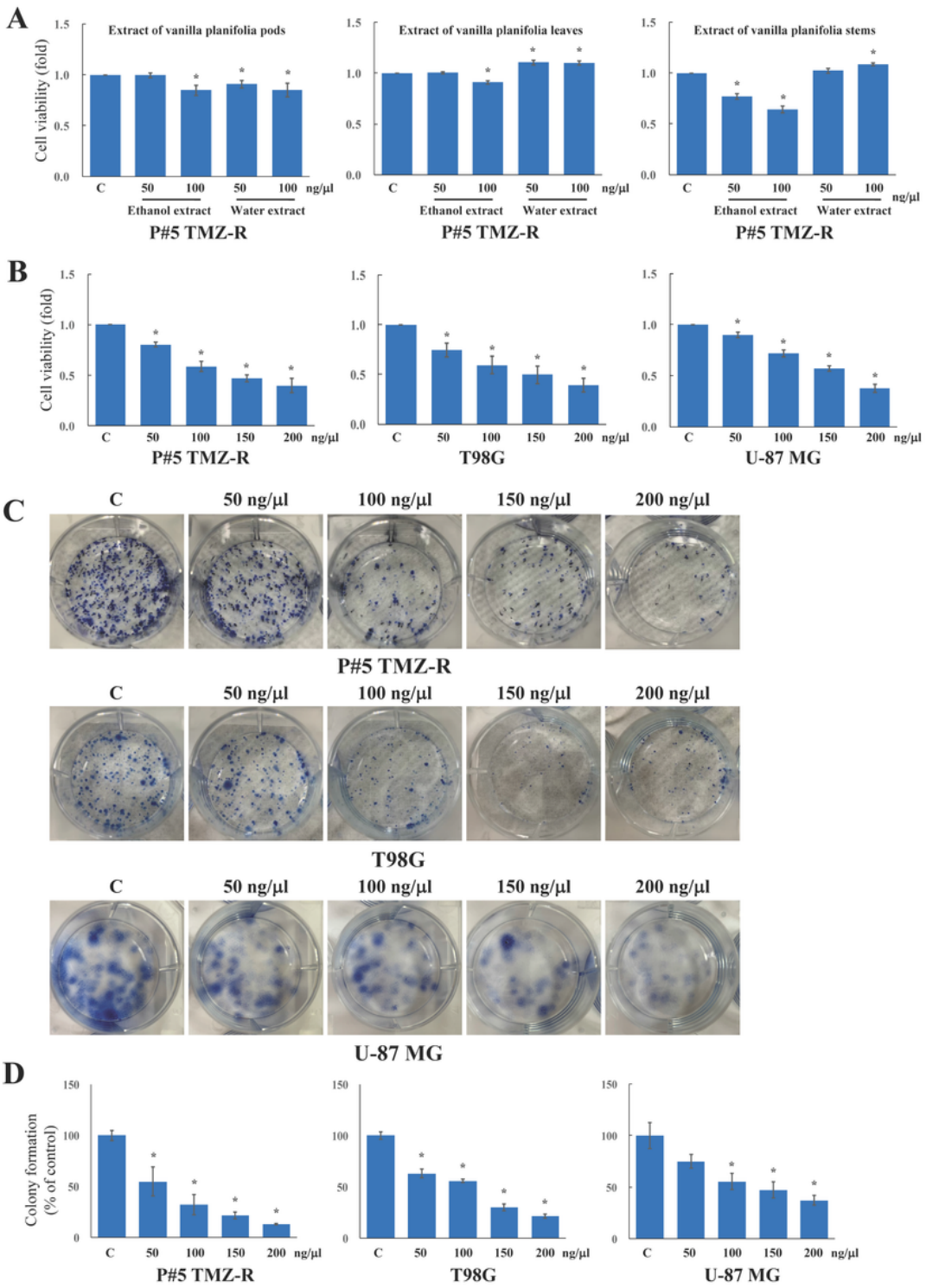

Figure 1

The antitumor effect of crude extract from vanilla planifolia on GBM cells. Cells were incubated with water extract and ethanol extract of vanilla planifolia pods, leaves, and stems at the indicated doses and then analyzed by cell viability assays (**A, B**) and clonogenic assays (**C**). The IC_{50} values were determined by plotting the growth relative to that of the vehicle controls. The quantification of colonies was

performed manually and compared to the vehicle control (**D**). All experiments were repeated at least three times. The data are expressed as the means ± SEM of three or more independent experiments. *p< 0.05.

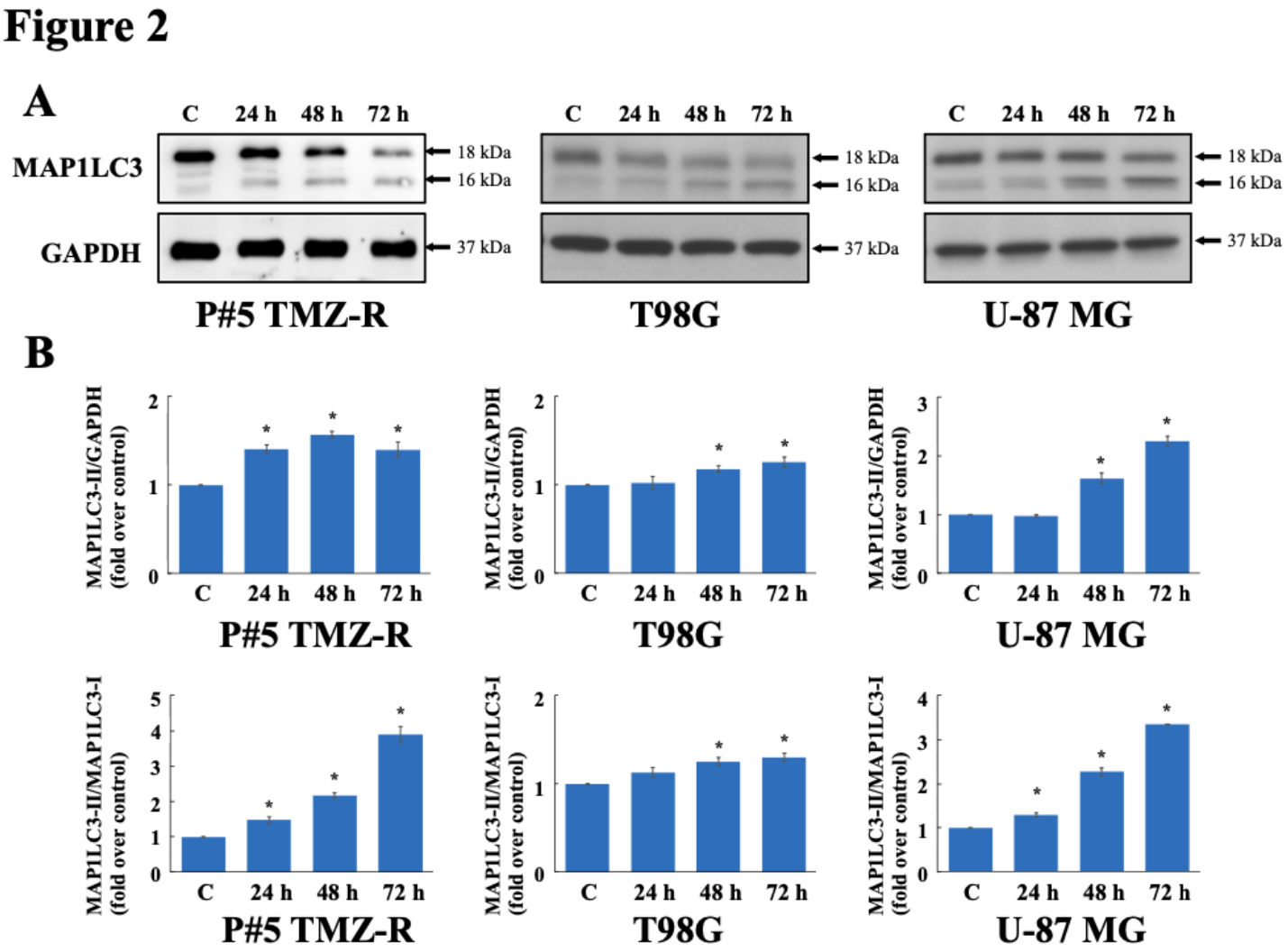

Figure 2

The effect of VAS on autophagy in GBM cells. Cells were incubated with 200 ng/ml VAS for the indicated times. The cells were analyzed by immunoblotting against specific antibodies (**A**). GAPDH was used as an internal control. The quantification of each band was shown in **B**. All experiments were repeated at least three times. The data are expressed as the means ± SEM of three or more independent experiments. *p< 0.05.

Figure 3

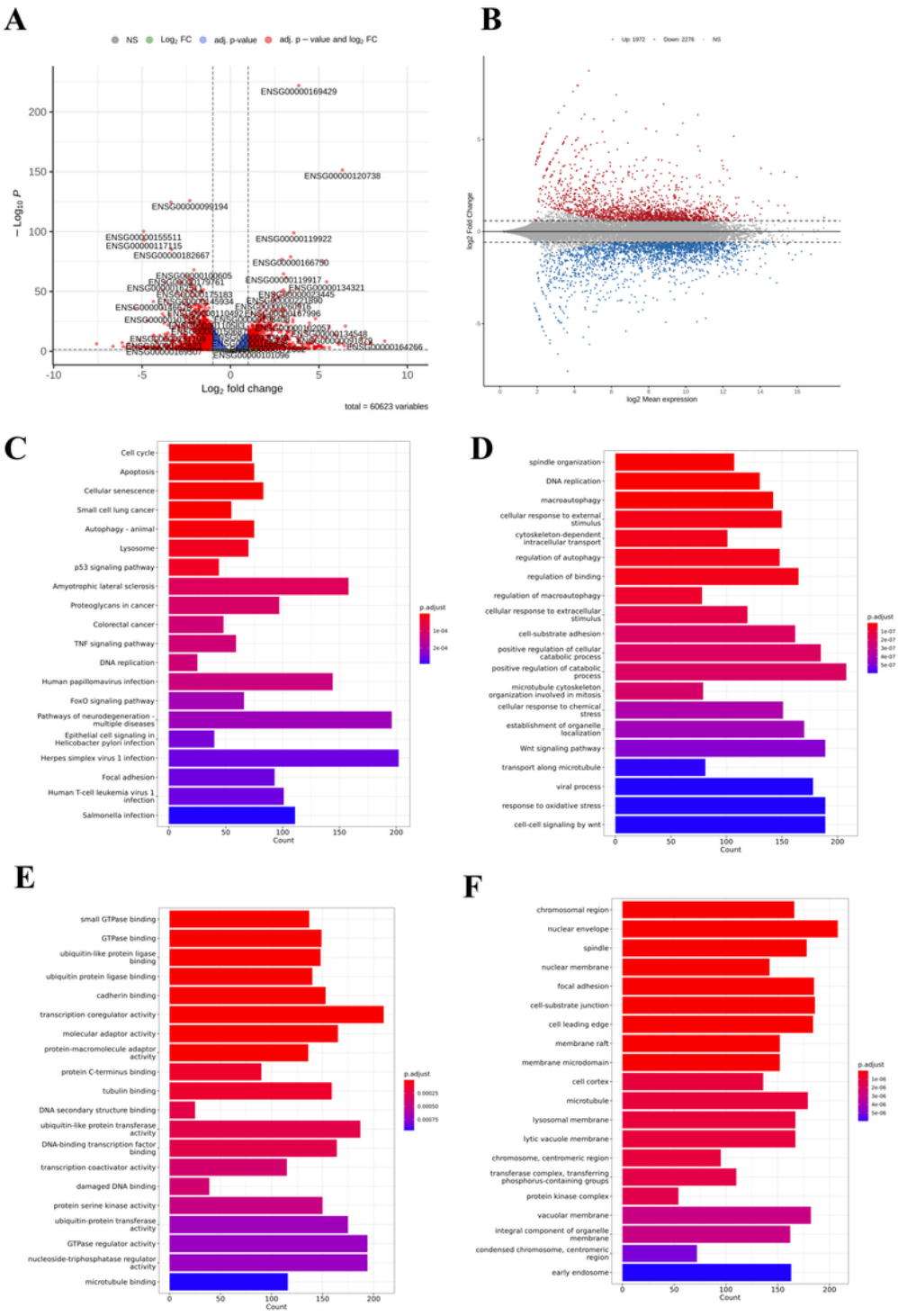

Figure 3

RNA-seq and DEG research after VAS treatment in terms of GO and KEGG. Volcano plot (**A**) and MA plot (**B**) of DEGs in P#5 TMZ-R cells treated with 200 ng/ml VAS for 72 hr. DEGs with p values below 0.05 were further analyzed by KEGG and GO. (**C**) The top 20 KEGG pathway analysis results of DEGs. (**D**) The top 20 biological process (BP) terms in the enrichment analysis. (**E**) The top 20 molecular function (MF)

terms in the enrichment analysis. (**F**) The top 20 cellular component (CC) terms in the enrichment analysis.

Figure 4

A **DEGs < -3**

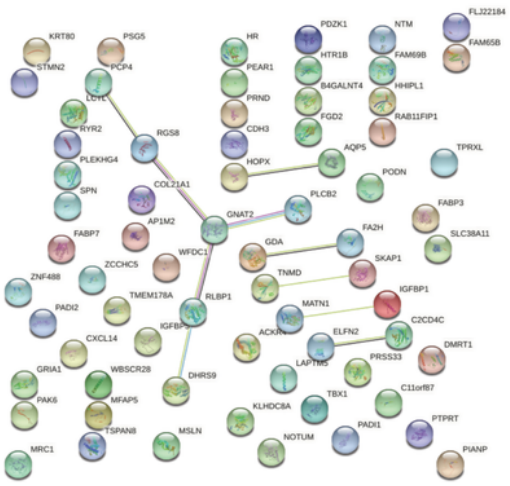

Gene	Fold Change (log2)
TNMD	-6.64
MATN1	-5.27
RLBP1	-4.78
IGFBP1	-4.36
PCP4	-4.24
DHRS9	-4.21
GNAT2	-4.07
C2CD4C	-3.82
ELFN2	-3.75
GDA	-3.70
AQP5	-3.56
SKAP1	-3.44
HOPX	-3.43
PLCB2	-3.24
FA2H	-3.24
RGS8	-3.19

C **DEGs > 5**

Gene	Fold Change (log2)
CXCL10	7.92
IL36RN	7.92
MX2	6.49
EGR1	6.33
RSAD2	5.44
CCL5	5.41
IFI44L	5.24
CCL20	5.19
HMOX1	5.18

Figure 4

Protein–protein interaction network of DEGs in GBM after VAS treatment. (**A**) Eight-nine DEGs were selected by the criteria of log2PostFC < -3 and p<0.05, and 16 DEGs were further selected by screening

their linkage to each other in the STRING database. (**C**) Twenty-three DEGs were selected by the criteria of log2PostFC > 5 and p<0.05, and 9 DEGs were selected by screening their linkage to each other in the STRING database. The fold change (log2) from RNA-seq of these hub DEGs is shown in **B** and **D**.

Figure 5

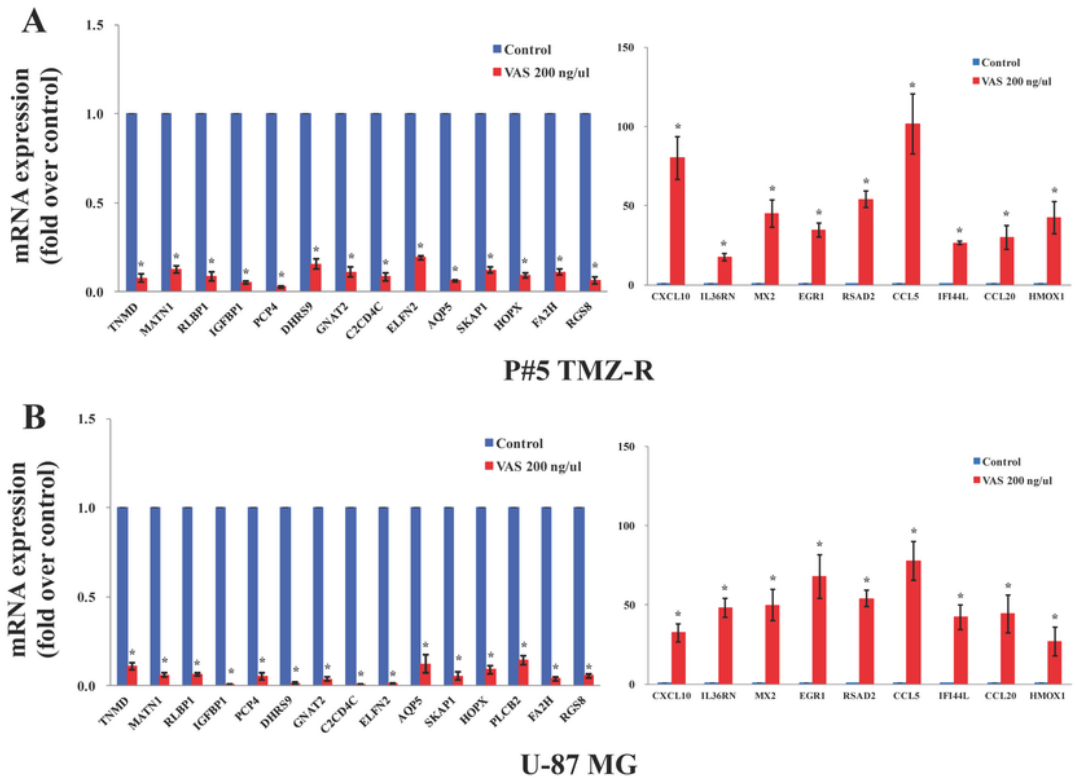

Figure 5

The mRNA expression of these hub DEGs in VAS-treated GBM cells. Cells were treated with VAS at 200 ng/ml for 72 hr, and then mRNA was harvested. The downregulated and upregulated mRNA expression levels of the hub DEGs mentioned above were confirmed in P#5 TMZ-R cells (**A**) and U-87 MG cells (**B**) by qPCR. GAPDH was used as an internal control for qPCR. The data are expressed as the means ± SEM of three or more independent experiments. *p< 0.05.

Supplementary Files

This is a list of supplementary files associated with this preprint. Click to download.

- TableS1.docx
- SupplementaryFigure1.tiff